International Journal of Electrospun Nanofibers and Applications
Vol.3 No. 1 (January, 2017)
ISSN : 0973-628X

Electrospinning of Chito-Oligosaccharide/ Poly(vinyl alcohol) Dissolved in Water

Orrawan Suthamnoi[a], Panu Danwanichakul[a]*, Piyawit Koombhongse[b], Surapich Loykulnant[b] & Oraphin Chaikumpollert[b]

[a]Department of Chemical Engineering, Faculty of Engineering, Thammasat University 99 Moo 18 Paholyothin Rd, Khlong Nung, Khlong Luang, Pathumthani 12120, Thailand

[b]National Metal and Materials Technology Center (MTEC), 114 Thailand Science Park, Paholyothin Rd., Khlong Nung, Khlong Luang, Pathumthani 12120, Thailand

Abstract: *Chitosan was depolymerized to chito-oligosaccharides (COS) with molecular weights of 14,000, 37,000 and 99,000 Da. The fabrication of COS nanofibrous structure was successful when using the blend COS/PVA (30,000-70,000 Da) in aqueous solutions. The average diameters were in the range of 57-200 nm. Bead-free fibers could be obtained at a high concentration of 30% and up to a COS/PVA ratio of 25/75 using COS with molecular weight of 14,000. For COS with molecular weights of 14,000 and 37,000, the average diameter decreased and more beads were seen with increasing the COS/PVA ratio. The opposite was seen for COS with molecular weight of 99,000. In addition, the negative electrode power supply was applied and compared with the positive one. It was found that when using the negative electrode power supply, for chiosan, which is a cationic polymer, the result was equivalent to lowering the magnitude of the electric field.*

Keywords: *Nanofiber, Electrospinning, chitosan, chito-oligosaccharide, poly(vinyl alcohol)*

1. INTRODUCTION

Chitosan is derived from chitin by removing the N-acetyl group on the copolymer consisting of β-(1→4)-2-acetamido-2-deoxy-D-glucopyranose and β- (1→4)-2-amino-2-deoxy-D-glucopyranose units. Due to its excellent properties including biocompatibility, biodegradability, and antibacterial activity, chitosan has been extensively found beneficial in many biomedical applications such as scaffolds and tissue engineering (Huang et al., 2005; Jiang *et al.*; 2006), and wound dressings to prevent fatal infections (Burkatovskaya *et al.*, 2006). High-molecular-weighted chitosan can be dissolved only in an acidic condition, and it is barely soluble at pH above 6.5. Recently, converting chitosan to chito-oligosaccharides (COS) has attracted much interest because oligosaccharides are not only water-soluble but they also have versatile biological properties, even better than high-molecular-weighted chitosan, such as antimicrobial activity (Jeon *et al.*, 2000) and antitumor activity (Prashanth &Tharanathan, 2005). To physically increase these activities of chitosan, several methods for fabricating nanostructures have been investigated, among which is electrospinning technique (Huang *et al.*, 2003).

[1]corresponding author: dpanu@engr.tu.ac.th

Electrospinning is an efficient technique known to produce polymer fibers in submicron scale. In this technique, the electric field is generated between the tip and the collector, inducing charges with repulsive interactions on the surface of spinning solution. When the electric field is increased until it equals to the surface tension of solution, the hemispherical drop at the tip is elongated to form a conical shape known as the Taylor cone. When the electric field overcomes the surface tension of solution, the charged jet is ejected from the tip of the Taylor cone and undergoes bending instability (Reneker *et al.*, 2000) and elongation process. The fiber becomes very long and thin while the solvent evaporates, leaving behind nonwoven nanofibers. There have been, thus far, many works investigating the effect of system parameters such as solution viscosity, surface tension, and conductivity and process parameters such as the applied electric field, the size of capillary tip and the distance between the tip and the collector. (Huang *et al.*, 2003)

Up to date, there have been many attempts to generate chitosan nanofibers by electrospinning but only Geng *et al.* (2005) was successful in electrospinning from chitosan solutions alone. They used chitosan with low degree of deacetylation (%DD) which is less than 65% in 90% (v/v) acetic solution. Other groups failed to do so–instead of nanofibers, the spherical particles were obtained. The inhibition of fiber formation might be from repulsive forces among ionic groups on chitosan molecules obstructing the entanglement of polymer chains, which is necessary for fiber formation. Therefore, many efforts have been made to fabricate chitosan nanofibers by indirect methods. For example, continuous chitosan fibers were deacetylated from electrospun chitin fibers, which was produced from the spinning solution of irradiated chitin in 1,1,1,3,3,3-hexafluoro-2-propanol (HFIP) (Min *et al.*, 2004). Another method is using blend solutions of chitosan and other easily fiber-forming polymers.

Many blends of chitosan with potential polymers have, therefore, been investigated. Park *et al.* (2004) fabricated nanofibers from silk fibroin (SF)/chitosan (CS) blend in formic acid solution. At a concentration of 11 wt% and a SF/CS ratio of 70/30, they could obtain nanofibers with an average diameter of 130 nm. Bhattarai *et al.* (2005) mixed chitosan and poly(ethylene oxide) or PEO in acetic/dimethylsulphoxide (DMSO) cosolvents and added triton X-100™ as a surfactant. At 2.2 wt% polymer concentration and a CS/PEO blend ratio of 10/90, ultrafine fibers having an average diameter of 38 nm were electrospun. In addition, chitosan was also blended with poly(vinyl alcohol) or PVA in acetic acid solutions and was electrospun (Li & Hsieh, 2006; Jia *et al.*, 2007). At the polymer concentration of 6 wt% and a PVA/CS ratio of 87/13, the produced fiber had an average fiber diameter of 100 nm. Derivatives of chitosan have also been studied. For instance, synthesized hexanoyl chitosan was electrospun to fibers with the diameters in the range of 0.64-3.93 μm using 4-14 wt% polymer concentration in chloroform (Neamnark *et al.*, 2006).

All works above utilized polymers in acidic or harmful solvents. These substances may not be completely removed from electrospun final products so they probably cause some side effects when applied medically. In the present work, to avoid using such hazardous solvents, water-soluble chitosan or COS is converted from high molecular weighted chitosan by a chemical reaction. Firstly, COS alone in aqueous solutions were

electrospun but the products were in particulate forms instead of nanofibrous structures. The work, thus, focuses on the electrospinning of COS/PVA blend in aqueous solutions because PVA is highly hydrophilic and able to easily form fibers, films and fiber mats. The effects of the polymer concentrations, the COS/PVA blend ratio, the COS molecular weight, and the electrode type of power supply on the morphology and the fiber diameter of the as-spun COS/PVA nanofibers were investigated.

2. EXPERIMENTAL

2.1 Materials

Chitosan from shrimp shells with 98% degree of deacetylation was obtained from A. N. LAB, Thailand. Poly(vinyl alcohol) (M_w = 30,000-70,000), cold watersoluble type was supplied from Sigma Aldrich. Sodium nitrite was purchased from Fluka. Sodium hydroxide (NaOH), acetone, and methanol were purchased from Labscan. Hydrochloric acid (HCl) was supplied from Merck. All chemicals were of analytical grade and used without further purification.

2.2 Chito-oligosaccharide (COS) Preparation

Chito-oligosaccharide was synthesized according to Allan and Peyron (1996). Initially, 2.0 wt% of chitosan was dissolved in 4 liters of 0.22 M HCl solution. The solution was heated to 60°C. For producing COS with different molecular weights, different amount (0.0552 g, 0.1104 g, or 0.552 g) of sodium nitrite was added and left reacted for 20 min. Afterwards, the pH of the reaction mixture was adjusted to 7 by adding 20 M aqueous NaOH solution gradually at room temperature. The sediment was, then, filtered by filter cloth three times and the remaining solution was evaporated until the volume was reduced to 500 ml. After that, COS was precipitated and washed with the 70% methanol solution twice. Finally, the washed product was dried in a vacuum oven at room temperature.

2.3 Spinning Solution Preparation and Electrospinning of Nanofibers

COS was blended with PVA in distilled water to obtain the spinning solutions with polymer concentrations of 10-30 %wt/vol and the weight ratios of COS to PVA of 100/0, 85/15, 75/25, 50/50, 25/75, 15/85 and 0/100.

The electrospinning apparatus was set up as shown in Fig 1. The spinning solution was poured into a 3 ml syringe with 0.65 mm-ID needle. The high voltage power supply (PS/MJ30PO400 Glassman) was connected to the end of the needle by a stainless steel electrode. Another electrode was connected to the stationary collector covered with aluminum foil. The electrospinning voltage was set at 18 kV and the distance between the needle tip and the collector was held constant at 9 cm. The spinning time was fixed at 5 min for each sample.

2.4 Measurement and Characterization

The average molecular weights, M_w, of the synthesized COS were measured with Gel Permeation Chromatography (PL-GPC 110) by using ultrahydrogel linear column and acetate buffer as a mobile phase.

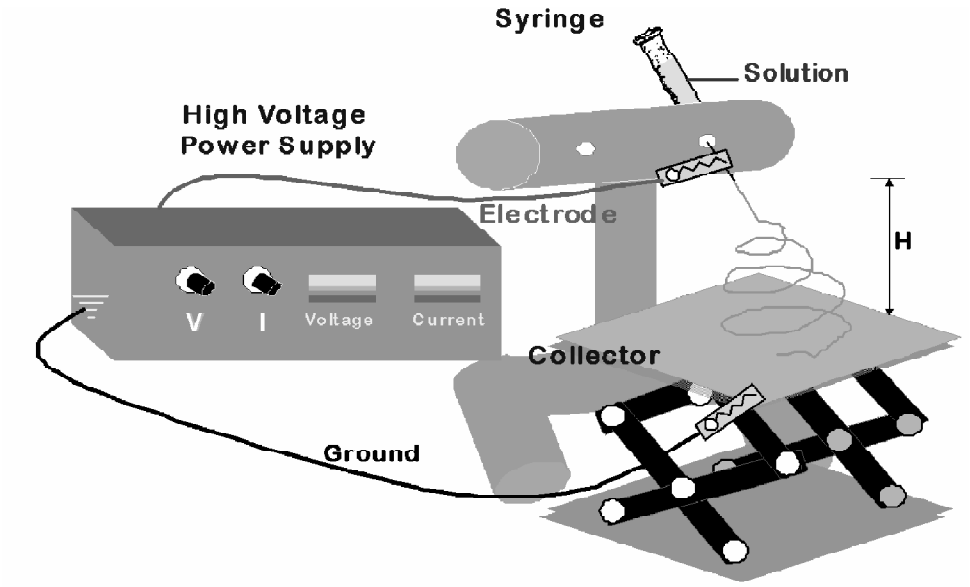

Figure 1: A Setup of Electrospinning Process

The dynamic viscosity of the COS/PVA solution was determined with Brookfield viscometer (programmable DV-II plus) at 25°C by using a spindle #21 and an 8-ml chamber. The surface tension of the blend solution was measured with a digital tensiometer (LAUDA-TD1) using Wilhelmy plate. The solution conductivity was measured with a conductivity meter (HORIBA ES-14).

The morphology of nanofibers was observed with Scanning Electron Microscope (SEM) (JEOL JSM-6310F) after gold coating by a gold sputtering coater for 100 seconds. The average fiber diameters were obtained with an image analyzer (Image-Pro Plus 4.5) by sampling at least 100 fibers. Fourier Transform Infrared FT-IR) spectra of electrospun fibers were recorded with Perkin Elmer system 2000 FT-IR spectroscopy (Imaging system) by using MCT detector in the range of 4,000-600 cm^{-1}.

3. RESULTS AND DISCUSSIONS

3.1 Solubility of Chito-oligosaccharide (COS) in Water

The molecular weights of synthesized COS samples were 14,000, 37,000 and 99,000 Da. The samples were named as COS14k, COS37k and COS99k, accordingly. The maximum solubility of each COS was determined to be 30, 12, and 7 % (wt/vol), respectively. Normally, the solubility increases upon decreasing molecular weight of a polymer. Besides, the maximum solubility of the cold-water-soluble PVA was more than 30%.

The solubility of each COS/PVA blend in distilled water was later tested. COS14k/PVA could be dissolved up to a total polymer concentration of 30% for all blend ratios. Since the solubility of COS is less than PVA, the solubility of the blend of these two

polymers will be decreased when increasing the weight ratio of COS. Therefore, at 30%, COS37k/PVA could be dissolved for a COS/PVA blend ratio up to 25/75, at 25%, up to 50/50 and at 10%, all blend ratios of polymers were soluble. The maximum solubility of COS99k/PVA was only 25% for a blend ratio up to 25/75. At 10%, the COS99k/PVA could be dissolved for a blend ratio up to 75/25.

3.2 Properties of Spinning Solutions

Properties of spinning solutions are shown in Figure 2, 3, and 4 for viscosity, surface tension and electrical conductivity, respectively. The results were obtained for the solutions which were not too viscous to be spun.

It can be seen in Figure 2 that viscosity increases drastically with polymer concentration, resulting from more friction drag on polymer molecules in water. This finding is the similar to the works of Jia *et al.* (2007), Min *et al.* (2004), and Park *et al.* (2004). Higher molecular weighted chitosan yields higher viscosity as was reported for chitosan dissolved in acetic acid solution (Geng *et al.*, 2005). The effect of the COS/PVA blend ratio is coupled with the effect of relative molecular weights of COS and PVA. As clearly seen, if the molecular weight of COS is greater than that of PVA, for example COS14k/PVA, the viscosity of the blend solution is higher for solutions with larger fraction of COS. On the contrary, if the molecular weight of PVA is greater than that of COS, for example COS99k/PVA, the viscosity of the blend solution is higher for solutions with larger fraction of PVA.

Figure 3 displays the measured surface tension of the spinning solutions. The polymer concentration, the molecular weight of COS, and the blend ratio of COS/PVA present similar effects on the solution surface tension. However, surface tension increases not as dramatically as viscosity with the polymer concentration.

The electronic conductivity of solution is shown in Figure 4. It is increased upon increasing the polymer concentration (Jia *et al.*, 2007; Park *et al.*, 2004) and seems to be smoothed out at an asymptote for a high polymer concentration, probably ascribed to the charge saturation from amino groups on COS chains. As the blend ratio of COS/PVA increases, there will be more protonated amino groups in the aqueous solution, thereby, increasing the conductivity. Besides, it was reported by Sandoval *et al.* (2005) that if the PVA fraction in blend solution increased, the interactions between chitosan and PVA would come from the hydrogen bonds between more hydroxyl groups of PVA and amino groups of chitosan in addition to the existing hydrogen bonds between hydroxyl groups of PVA and hydroxymethyl of chitosan, resulting in smaller number of charges.

The effect of COS molecular weight on the solution conductivity is not obvious. The conductivity results from the degree of protonation on COS chains. In a dense polymer solution, the chains are entangled together. In case of longer chains of PVA and shorter chains of COS, the chain connection comes mainly from PVA by hydrogen bonds. Usually, the interactions between hydroxyl groups of PVA and hydroxymethyl groups of chitosan are more energetically favorable than those between hydroxyl groups of PVA and amino groups of chitosan (Sandoval *et al.*,2005) Therefore, the interactions of the remaining hydroxyl groups of PVA molecules and hydroxymethyl groups of COS are preferable,

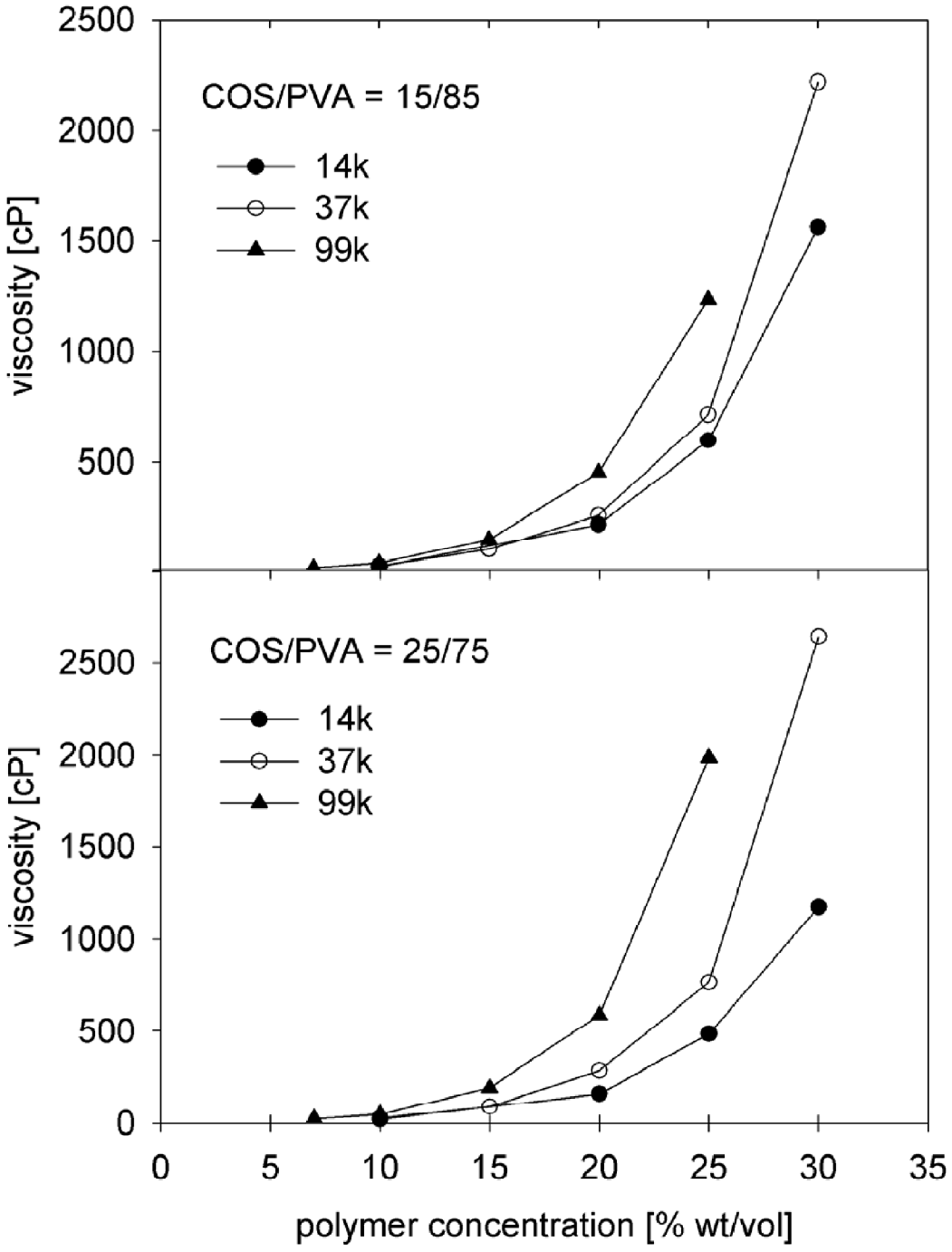

Figure 2: The Viscosity of COS/PVA Solutions Showing the Effect of the Polymer Concentration, the COS/PVA Weight Ratio, and the Molecular Weight

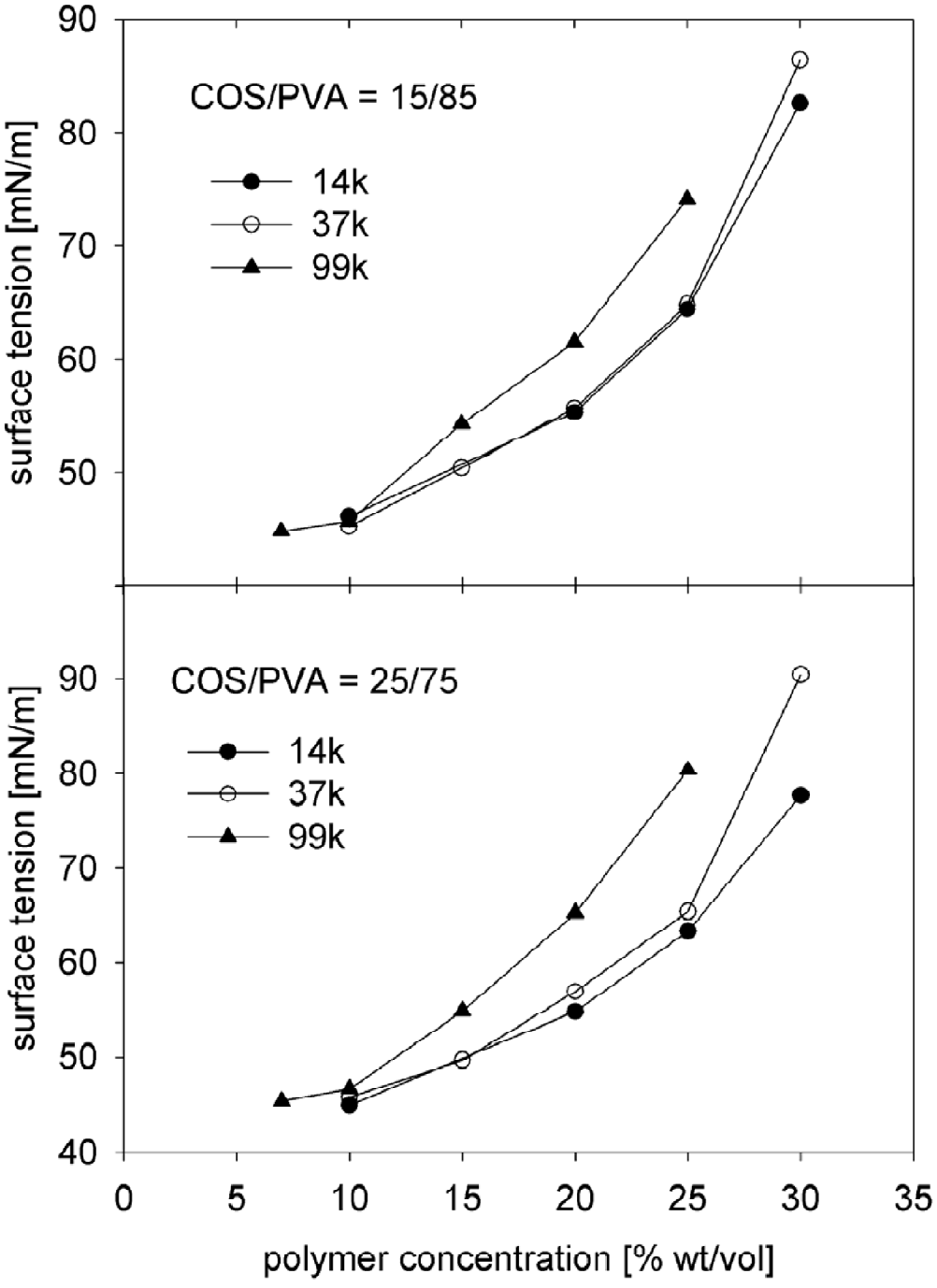

Figure 3: The Surface Tension of COS/PVA Solutions Showing the Effect of the Polymer Concentration, the COS/PVA Weight Ratio, and the Molecular Weight

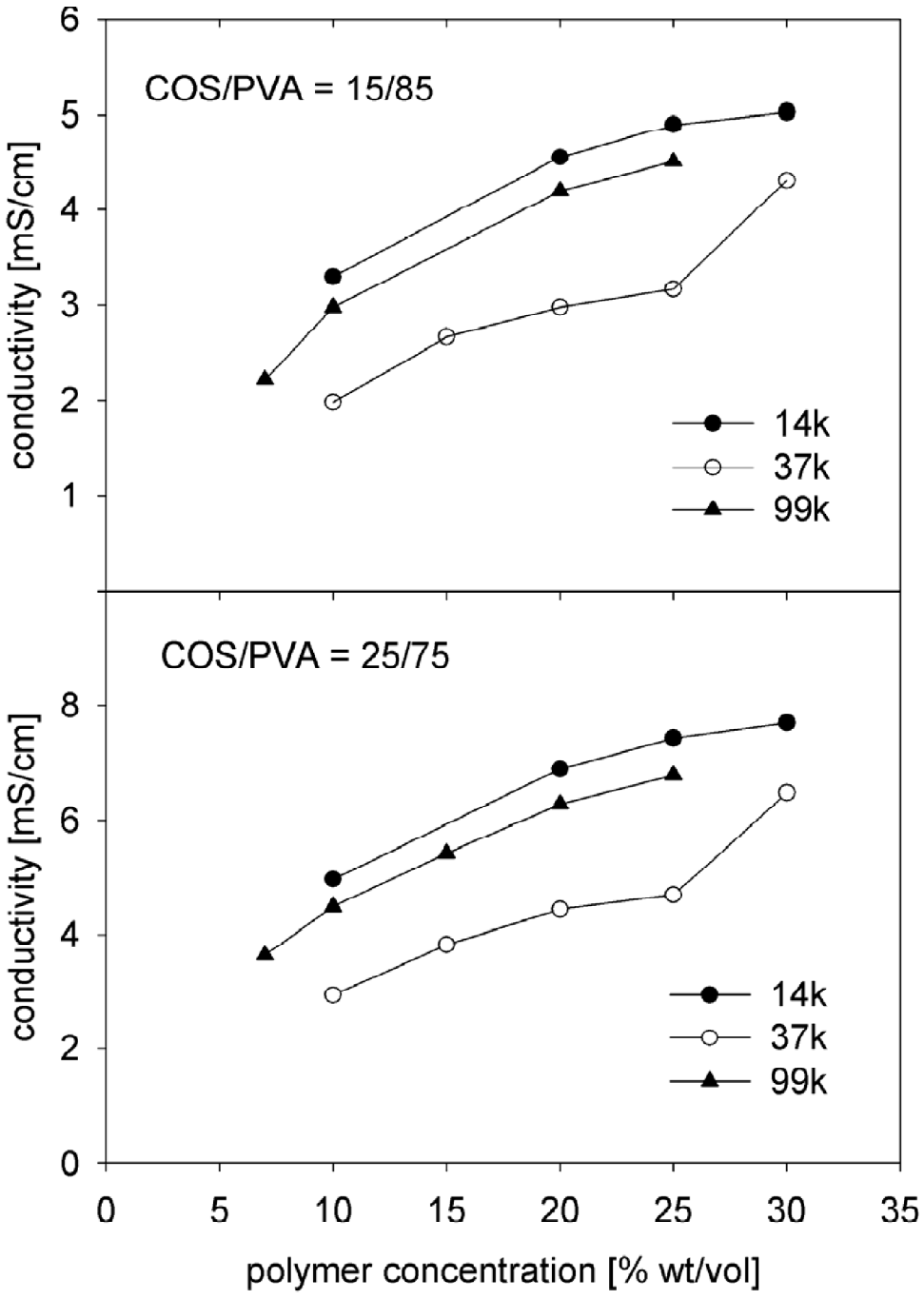

Figure 4: The Electronic Conductivity of COS/PVA Solutions Showing the Effect of the Polymer Concentration, the COS/PVA Weight Ratio, and the Molecular Weight

leaving the amino groups to be freely charged. This case gave the highest conductivity. In case of longer chains of COS and shorter chains of PVA, PVA molecules facilitate entanglements between COS chains by shielding the repulsive forces between cations on COS molecules. This increases the possibility for the interactions between functional groups to occur, leading to less number of amino groups to be freely charged. If the chains of PVA and COS are about the same length, the entanglements would be equally probable from hydroxymethyl and amino groups of COS. Consequently, this case yielded the lowest conductivity.

3.3 Effect of the Polymer Concentration on Morphology

Figure 5 shows the effect of polymer concentration on the morphology of the electrospun fibers when the COS14k/PVA blend ratio was fixed at 15/85. The positive electrode power supply was used. As can be seen, at 10% wt/vol particles were electrodeposited on the surface instead of nanofibers. According to Mckee *et al.* (2004), chain entanglement is a key factor in the formation of nanofibers. The polymer concentration has to be greater than the entanglement concentration, C_e, which is the boundary between the semidilute un-entangled regime and the semidilute entangled regime. In this case, at 10%, the number of entanglement was not enough to sustain spinning of continuous fibers. The transformation of beads to fibers was seen at 20% as bead-string fibers with the fiber average diameter between beads of 61nm. At a higher concentration of 25%, the fibers with few beads were seen while at 30%, the smooth and uniform fibers were produced. Our results were somewhat close to what suggested by Mckee *et al.* (2004), which was stated that the concentration of 2.0-2.5 times C_e was the minimum concentration aimed for bead-free fibrous structures.

The average diameter of nanofibers from 25% and 30% solutions were 95 and 118 nm, respectively. Figure 2 and Figure 4 show that the solution viscosity and conductivity increase with the solution concentration. While the electrical force elongates the fibers, the viscoelastic force holds back the stretching of fibers. In this study, it seemed that the effect of viscosity was dominant so that the average size of nanofibers increased with the solution viscosity, similar to the results of produced chitosan/PVA nanofibers (Jia et al, 2007) and collagen/PVA nanofibers (Chen *et al.*, 2007).

3.4 Effect of the COS/PVA Blend Ratio on Morphology

The results for COS14k, COS37k, and COS99k, are illustrated in Figure 6, 7, and 8, respectively. These results were from solutions at the maximum solubility which is 30% for COS14k and COS37k, and 25% for COS99k. The positive electrode power supply was used.

For COS14k/PVA at 30%, the nanofibrous structures could be generated as bead-on-string fibers for the COS14k/PVA blend ratio of 50/50 and as uniform fibers for blend ratios of 15/85 and 25/75. The effect of viscoelastic force from viscous solution is responsible for getting smooth and larger fibers. This effect increased with PVA fraction for COS14k as was discussed already in Section 3.3. If the fraction of chitosan was greater than 50%, the particles were deposited instead. This finding is consistent with

what was observed by Jia *et al.* (2007) and Li & Hsieh (2006). In addition, smaller sizes of particles were seen when increasing the fraction of chitosan, implying that the repulsive interactions between chitosan molecules increased with the amount of chitosan. When PVA was less than 50%, it could not shield the repulsive forces between chitosan molecules, resulted in inhibiting the chain entanglement which is necessary for initiating fiber formation.

For COS37k at 30% and COS99k at 25%, the uniform fibers could not be obtained. Instead, the beaded fibers were produced up to a COS/PVA ratio of 25/75, above which sprayed particles were produced. Like COS14k/PVA blend, the average diameter of COS37k/PVA blend fibers and the number of beads increased with the solution viscosity which was increased upon increasing COS content. Even though the conductivity was also increased as COS content increased, the effect of viscosity seemed to be more significant. However, for COS99k, the average size of fiber was not much different and the number of beads was fewer when increasing COS content from 15/85 to 25/75 even though the viscosity was increased. So in this case, the effect of conductivity was dominant.

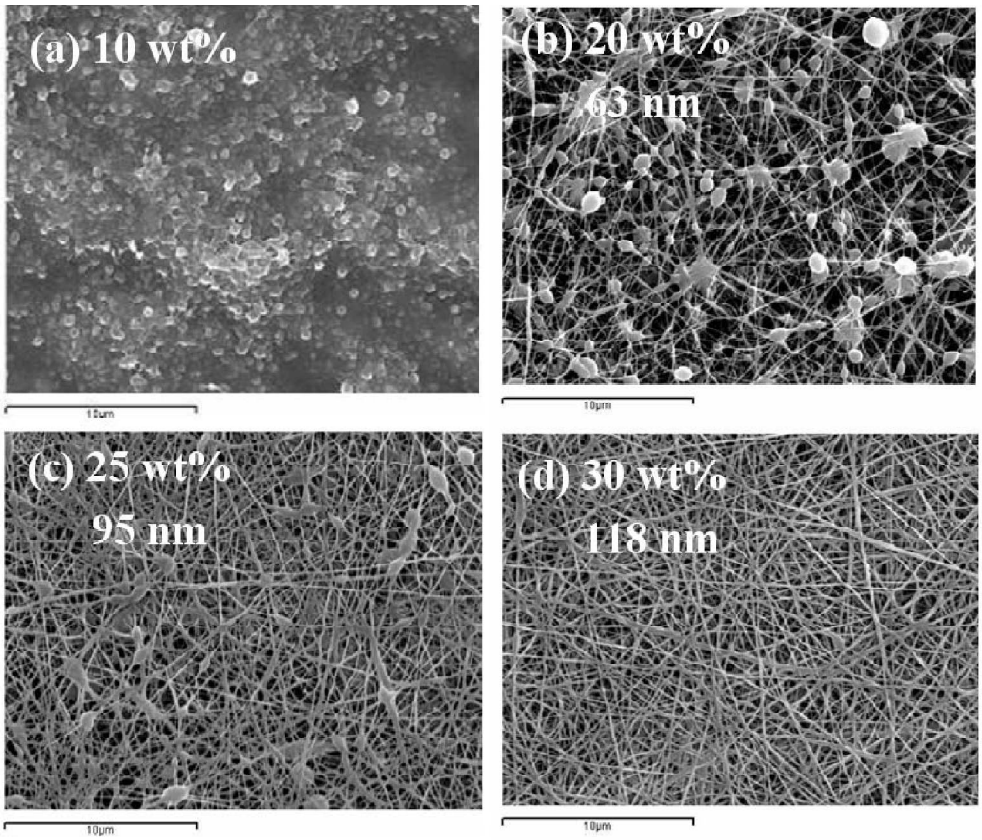

Figure 5: SEM Micrographs of the COS14k/PVA Electrospun Products at Different Polymer Concentrations and the Fixed Blend Ratio of 15/85, using the Positive Electrode Power Supply

3.5 Effect of the COS Molecular Weight on Morphology

In addition to Figures 6 and 7 which show the results of COS14k and COS37k, respectively at the concentration of 30%, Figure 9 displays the comparison of the morphology of the electrospun fibers using different COS molecular weights for a polymer concentration of 25% and a COS/PVA ratio of 15/85. The positive electrode power supply was used.

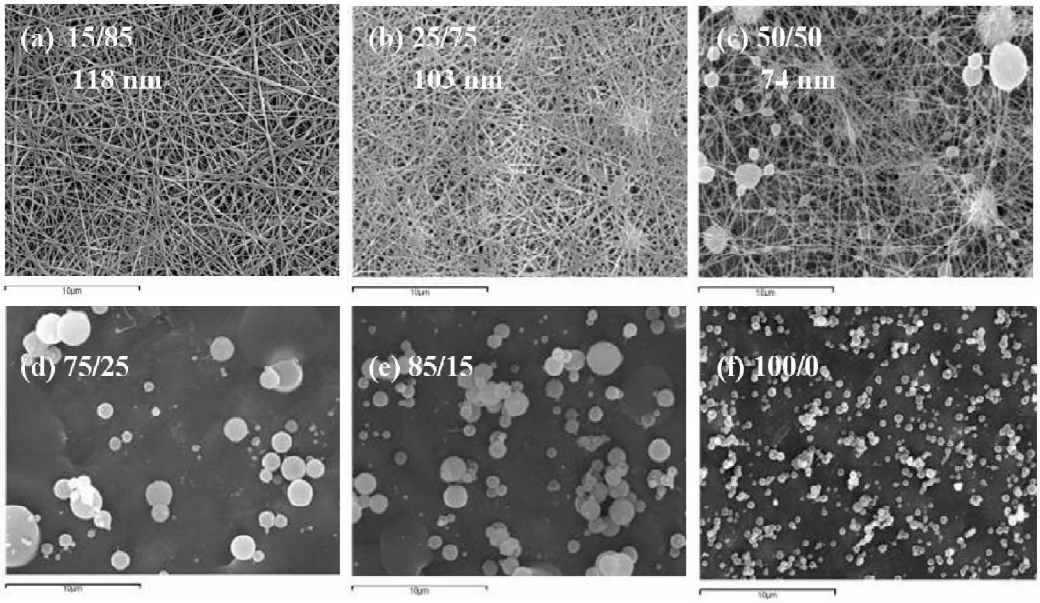

Figure 6: SEM Micrographs of the COS14k/PVA Electrospun Products at Different Blend Ratios and the Fixed Polymer Concentration of 30 wt%, using the Negative Electrode Power Supply

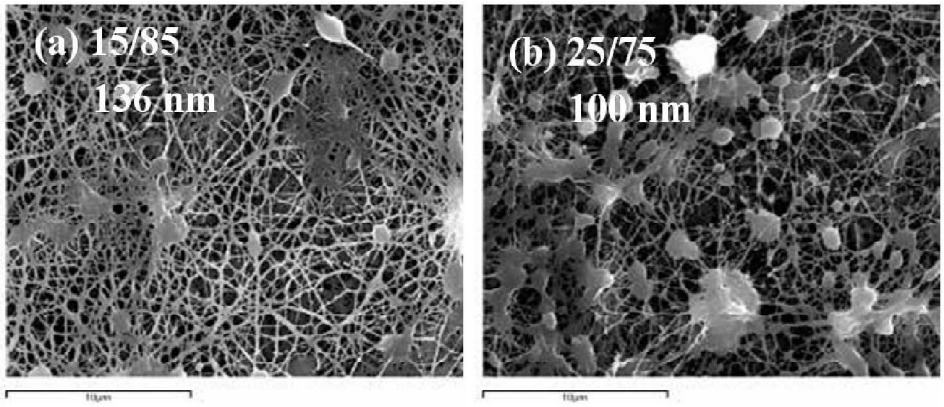

Figure 7: SEM Micrographs of the COS37k/PVA Electrospun Fibers at Different Blend Ratios of 15/85 and 25/75 and the Fixed Polymer Concentration of 30 wt%, using the Negative Electrode Power Supply

The most uniform fibers were obtained when using COS14k, which was better than using COS99k. Fibers were hardly electrospun from COS37k. It is possible that the conductivity of the solution, which is from the protonation of amino groups on COS molecules, is lower if there are more interactions between hydroxyl groups on PVA chains with amino groups of chitosan. The data in Figure 4 shows that the conductivity of COS14k solution is greater than COS99k and COS37k solutions, respectively. This suggests that when compared with other COSs, the entanglements of PVA and COS37k chains result from more number of interactions between hydroxyl groups of PVA and amino groups of chitosan. As studied by molecular dynamics simulations (Sandoval *et al.*, 2005), the interactions between hydroxyl and hydroxymethyl groups are stronger than hydroxyl and amino groups. When the solution is electrospun, the entanglements originated from hydroxyl-amino groups interactions will be more easily to break. Therefore, when using the polymer concentration of 25%, COS14k solution yielded the best fiber formation while COS37k solution could not be used to form fibers. However, as shown in Figure 7, COS37k/PVA could be electropun to nanofibers at 30% polymer concentration, but the quality was lower than COS14k/PVA fibers.

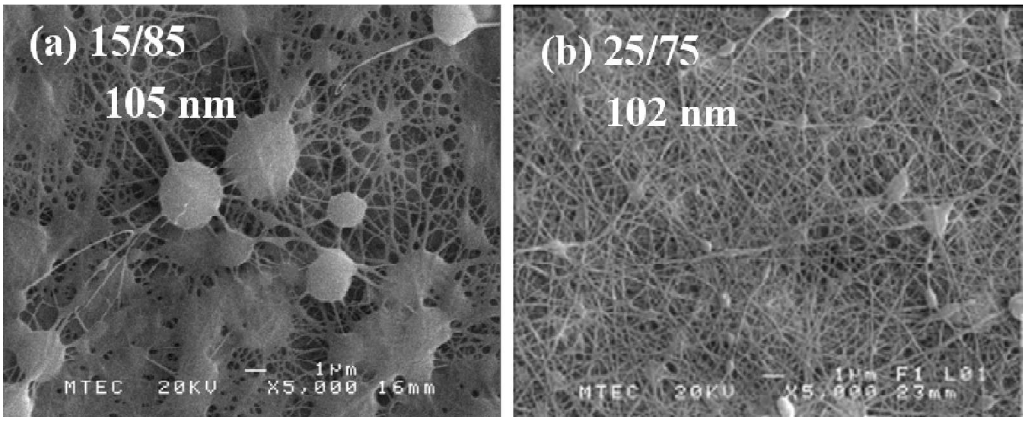

Figure 8: SEM Micrographs of the COS99k/PVA Electrospun fibers at Different Blend Ratios of 15/85 and 25/75 and the Fixed Polymer Concentration of 25 wt%, using the Negative Electrode Power Supply

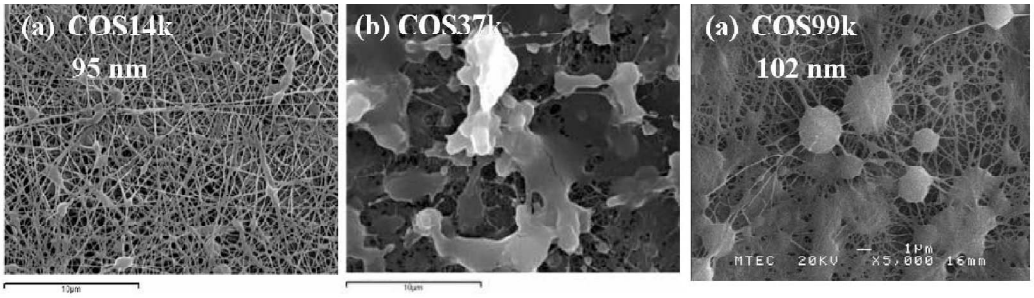

Figure 9: SEM Micrographs of the COS/PVA Electrospun Products at a Polymer Concentration of 25 % and a COS/PVA Ratio of 15/85, Comparing the Effect of the COS Molecular Weight

3.6 Effect of the Electrode Type on Morphology

The effect of the electrode type of high-voltage power supply, i.e. the negative and the positive electrodes, was also investigated by using a COS14k/PVA ratio of 15/85. The comparison could be made between Figure 5 for the positive electrode and Figure 10 for the negative electrode.

At all concentrations, the negative electrode power supply gave fibers with larger average diameter than positive electrode. Evidently, the negative electrode power supply generated less force than the positive one, due to less net charge density on the surface of fibers during spinning process. Chitosan in the aqueous solution is a cationic polymer. When counteracting with the negative charges produced by the negative electrode power supply, this will lead to less repulsive force to stretch the fiber. For both electrodes, the fiber diameter was larger and the number of beads was less when using higher polymer concentration. This was from the effect of viscosity counterbalanced with the electric forces. Obviously, at 30 wt% concentration, when using the negative electrode, only a few fibers were fabricated, possibly, because the effect of net charge density was nearly unable to overcome the effect of viscosity which was too high in this case.

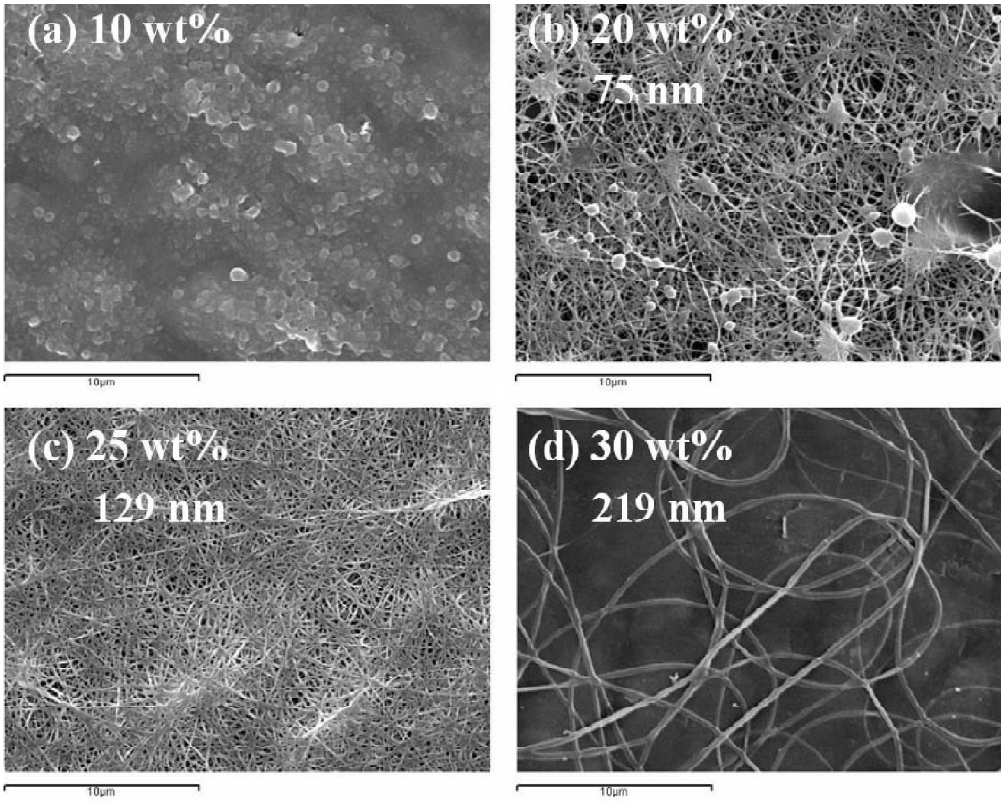

Figure 10: SEM Micrographs of the COS14k/PVA Electrospun Products at Different Polymer Concentrations and the Fixed Blend Ratio of 15/85, using the Negative Electrode Power Supply

3.7 FT-IR Spectra

Figure 11 shows the FT-IR spectra of COS, PVA, and COS/PVA nanofibrous structures. The spectra of COS nanofibers exhibits the resonance bands at 1630, 1528, and 3405 cm^{-1}, which represents the carbonyl stretching of the secondary amide band (amide I), the N-H bending of the primary amino group, and the N-H stretching peak, respectively. The PVA nanofibers shows a number of absorption peaks at 3346, 2942, and 1735 cm-1, which are attributed to the O-H stretching, the C-H stretching and the residual carbonyl acetyl group, respectively.

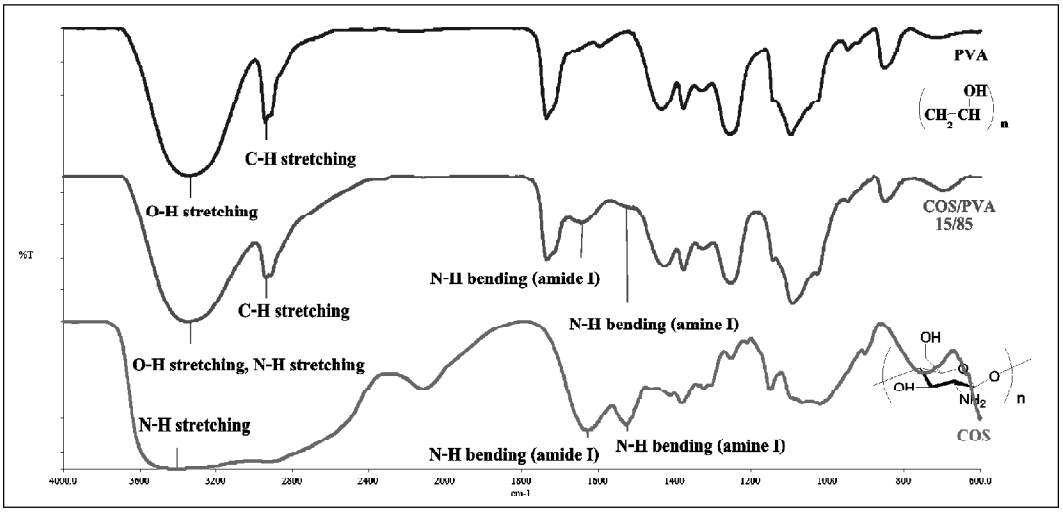

Figure 11: FT-IR Spectra of the PVA, COS/PVA Blend and COS Electrospun Nonfibers; COS14k, polymer concentration = 30 wt% and COS/PVA = 15/85

The absorption peaks of the electrospun COS/PVA fibers (30 wt% concentration and COS/PVA = 15/85) are observed at 3349 cm^{-1} owing to both the OH stretching of PVA and the N-H stretching of COS. Moreover, the C-H stretching and the residual carbonyl acetyl group of PVA spectra appears at 2941 and 1736 cm^{-1} and the carbonyl stretching of the secondary amide band (amide I) and the N-H bending of the primary amino group of COS spectra are seen at 1645 and 1525 cm^{-1}, respectively.

4. CONCLUSIONS

Chito-oligosaccharides (COS) were synthesized. The three molecular weights of COS, which are 14,000, 37,000 and 99,000 Da, were experimented by mixing with PVA in distilled water. The COS/PVA electrospun nanofibers were successfully fabricated. The average fiber diameter was in the range of 57-200 nm which was smaller than PVA fibers (90-260 nm, not displayed here). However, the larger average fiber diameter was obtained at a higher concentration. The bead-free fibers could be produced from the solution with a concentration as high as 30% and a COS/PVA blend ratio of 25/75 when using COS14k/PVA blend. The nanofibrous structures of COS37k/PVA could not be obtained

for polymer concentration less than 30% and only bead-on-string fibers could be produced. For COS14k/PVA and COS37k/PVA, the average diameter of nanofibers decreased and more beads were present with increasing the COS/PVA ratio, whereas, for COS99k/PVA, fewer beads were obtained and fiber size was not much different.

The interesting results were found when comparing the results for the positive and negative electrode power supplies. The negative electrode power supply could generate uniform fibers at a lower concentration of 10% because the effect of viscosity could dominate the effect of solution conductivity. Finally, FT-IR spectra of COS/PVA blend nanofibers was checked to confirm that both COS and PVA were the components in those fibers. In order to apply this composite for wound dressing and scaffold applications, the nanofiber mats have to be crosslinked to increase the stability in water. This is being investigated by our groups.

ACKNOWLEDGEMENT

This research was financially supported by the National Metal and Materials Technology Center (MTEC). O. Suthamnoi would like to acknowledge the scholarship from Thailand Graduate Institute of Science and Technology (TGIST) (TG-33-13-850-M). P. Danwanichakul is greateful to the Office of National Research Council of Thailand for a partial financial report.

References

[1] Allan, G., & Peyron, M. (1997), Depolymerization of Chitosan by Means of Nitrous Acid. In R. A. Muzzarelli & M. G. Peter (Eds). *Chitin Handbook* (pp. 175-179). Seattle, USA: European Chitin Society.

[2] Bhattarai, N., Edmondson, D., Veiseh, O., Matsen, F. A., & Zhang, M. (2005), Electrospun Chitosan-based Nanofibers and their Cellular Compatibility. *Biomaterial*, 26, 6176-6184.

[3] Burkatovskaya, M., Tegos, G. P., Swietlik, E., Demidova, T. N., Castano, A. P., & Hamblin, M. R. (2006), Use of Chitosan Bandage to Prevent Fatal Infections Developing from Highly Contaminated wounds in mice. *Biomaterials*, 27, 4157-4164.

[4] Chen, Z., Mo., X., Qing, F. (2007), Electrospinning of Collagen-chitosan Complex. *Materials Letters*, 61, 3490-3494.

[5] Geng, X., Kwon, O. H., & Jang, J. (2005), Electrospinning of Chitosan Dissolved in Concentrated Acetic Acid Solution. *Biomaterial*, 26, 5427-5432.

[6] Prashanth, K.V. H., & Tharanathan, R. N. (2005), Depolymerized Products of Chitosan as Potent Inhibitors of Tumor-induced Angiogenesis. *Biochimica et Biophysica Acta*, 1722, 22-29.

[7] Huang, Y., Onyeri, S., Siewe, M., Moshfeghian, A., & Madihally, S.V. (2005), In Vitro Characterization of Chitosan-gelatin Scaffolds for Tissue Engineering. *Biomaterials*, 26, 7616-7627.

[8] Huang, Z. M., Zhang, Y. Z., Kotaki, M., & Ramakrishna, S. (2003), A Review on Polymer Nanofibers by Electrospinning and their Applications in Nanocomposites. *Composites Science and Technology*, 63, 2223-2253.

[9] Jeon, Y. J., Park, P. J., & Kim, S. K. (2000), Antimicrobial Effect of Chitooligosaccharides Produced by Bioreactor. *Carbohydrate Polymer*, 44, 71-76.

[10] Jia, Y. T., G., Gong, J., Gu, X. H., Kim, H. Y., Dong, J., & Shen, X. Y. (2007), Fabrication and Characterisation of Poly(vinyl alcohol)/chitosan blend Nanofibers Produced by Electrospinning Method. *Carbohydrate Polymers*, 67, 403-409.

[11] Jiang, T., Abdel-Fattah, W. I., & Laurencin, C. T. (2006), In Vitro Evaluation of Chitosan/ poly (lactic acid-glycolic acid) Sintered Microsphere Scaffolds for Bone Tissue Engineering. *Biomaterials*, 27, 4894-4903.

[12] Li, L., & Hsieh, Y. L. (2006), Chitosan Biocomponent Nanofibers and Nanoporous Fibers. *Carbohydrate Research*, 341, 374-381.

[13] Mckee, M. G., Wilkes, G. L., Colby, R. H., & Long, T. E. (2004). Correlations of Solution Rheology with Electrospun Fiber Formation of Linear and Branched Polyesters. *Macromolecules*, 37, 1760-1767.

[14] Min, B. M., Lee, S. W., Lim, J. N., You, Y., Lee, T. S., Kang, P. H., & Park, W. H. (2004), Chitin and Chitosan Nanofibers: Electrospinning of Chitin and Deacetylation of Chitin Nanofibers. *Polymer*, 45, 7137-7142.

[15] Neamnark, A., Rujiravanit, R., & Supaphol, P. (2006), Electrospinning of Hexanoyl Chitosan. *Carbohydrate Polymers*, 66, 298-305.

[16] Park, W. H., Jeong, L., Yoo, D. I., & Hudson, S. (2004), Effect of Chitosan on Morphology and Conformation of Electrospun Silk Fibroin Nanofibers. *Polymer*, 45, 7151-7157.

[17] Reneker, D. H., Yarin, A. L., Fong, H., & Koombhongse, S. (2000), Bending Instability of Electrically Charged Liquid Jets of Polymer Solutions in Electrospinning. *Journal of Applied Physics*, 87, 4531-4547.

[18] Sandoval, C., Castro, C., Gargallo, L., Radic, D., & Freire, J. (2005), Specific Interactions in Blends Containing Chitosan and Functionalized Polymers. Molecular Dynamics Simulations, *Polymer*, 46, 10437-10442.